Desalination and Water Treatment
www.deswater.com

doi: 10.5004/dwt.2017.21357

89 (2017) 240–249
September

Kinetics, equilibrium and thermodynamics of cerium removal by adsorption on low-rank coal

Tariq Javed[a,*], Nasir Khalid[b], Muhammad Latif Mirza[a]

[a]*Department of Chemistry, The Islamia University of Bahawalpur, Bahawalpur, Pakistan, Tel. +92 3455652137; Fax +92 5449270462; email: jtariq56@yahoo.com (T. Javed), Tel. +92 3026825055; email: mlatifmirza@yahoo.com (M.L. Mirza)*
[b]*Chemistry Division, Pakistan Institute of Nuclear Science and Technology, Islamabad, Pakistan, Tel. +92 3335154870; email: nasirk1953@gmail.com*

Received 17 January 2017; Accepted 22 August 2017

ABSTRACT

The removal of cerium ions on low-rank coal has been studied as a function of contact time, nature of electrolytes ($HClO_4$, HCl, H_2SO_4 and HNO_3), dose of adsorbent, metal ion concentration and temperature. The radiotracer technique was applied to examine the distribution of cerium (Ce^{3+}) using a batch method. Maximum adsorption was found to be at pH 5, using 0.4 g of adsorbent for 4 mL of 5 mg L^{-1} cerium concentration with equilibration time of 25 min. The adsorption of cerium was decreased with the increase in the concentrations of all the mineral acids used. The kinetic data indicated an intraparticle diffusion process with adsorption being pseudo-second order. The examined rate constant K_2 was 25 g mg^{-1} min^{-1}. The adsorption data obeyed the Langmuir, Freundlich and Dubinin–Radushkevich isotherm plots over the cerium concentration range of 7.137×10^{-3} to 6.423×10^{-4} mol L^{-1}. The characteristic Freundlich constants, that is, $1/n = 0.381$ and $K = 5.152 \times 10^{-2}$ m mol g^{-1} whereas the Langmuir constants $Q = 2.889 \times 10^{-3}$ m mol g^{-1} and $b = 14.072 \times 10^{3}$ dm^3 mol^{-1} have been calculated for the adsorption system. The adsorption mean free energy from the Dubinin–Radushkevich isotherm is 12.987 kJ mol^{-1} indicating chemical adsorption of ion-exchange mechanism. The uptake of cerium was increased with the rise in temperature (283–333 K). Thermodynamic quantities, that is, ΔH, ΔG and ΔS have been computed and discussed for the system. Adsorbent was characterized by using scanning electron microscopy and Fourier transform infrared spectroscopy before and after the adsorption of cerium. Effect of coexistent ions on the adsorption of cerium has also been investigated. Removal of cerium from tap water sample shows that the proposed method is successfully applicable.

Keywords: Low-rank Pakistani coal; Cerium adsorption; Kinetics; Isotherms; Thermodynamics

1. Introduction

The presence of toxic metals and radionuclides in wastes is of main environmental concern that attracted the attention of researchers in these days. Radioisotopes in radioactive waste are considered hazardous pollutants, and their movement with groundwater is affected by adsorption on the geologic materials [1]. Cerium is one of the most abundant elements of the lanthanide series having about 66 ppm in the earth's crust. Cerium is also present along with other rare earth elements in its minerals as well as in spent nuclear fuel. The most important uses of cerium include the production of super conductors and super magnets, catalyst support, chips and computer hard disks, polishing powders, optic fibers, laser industry, controllers of nuclear reactors, preparation of scintillation counters and production of radiopharmaceuticals [2–5].

The effluents of all these activities contain the harmful radionuclides including cerium, which makes it essential to separate these radio toxicants from aqueous media before their safe disposal into water bodies. Once absorbed in human body, cerium tends to accumulate primarily in the

* Corresponding author.

bones, liver, heart and lungs. The harmful effects of cerium include interstitial lung disease and pneumoconiosis, threat to liver, chromosomal break and cardiac effects [6–9].

Different techniques such as chemical precipitation [10], solvent extraction [11–13], ion-exchange [14], coagulation [15], flotation [16,17], solvent sublation [17,18] and adsorption have been reported for the separation of cerium ions from aqueous media. The practical application of all these methods is limited due to lack of specificity, high operational costs, generation of huge hazardous sludge or low efficiency especially at low concentrations. Therefore, there is a need to develop cost-effective, simple, rapid and efficient procedure. The adsorption process under certain conditions has a definite edge over other methods due to its simplicity, high enrichment factor, rapid phase separation and low maintenance cost.

Various scientists had used different adsorbents for the removal of cerium ions from aqueous media. The adsorbents used are *Pinus brutia* leaf powder [19], *Platanus orientalis* leaf powder [20], calcium alginate beads [21], polyethylene films [22], tangerine (*Citrus reticulata*) peel [23], kaolin clay [24], activated carbon [25], metal oxides [26,27] and bentonite [28].

The present work deals with the exploitation of the potential of low-rank Pakistani coal as an adsorbent for the removal of cerium from wastewater. The material was selected since it is abundantly available as a low cost material even after its wide consumption as a fuel in power generation plants, brick kilns and other industries. The low-rank Pakistani coal possesses a grainy structure, having oxygenated carboxyl and phenolic hydroxyl functional groups which have the capability to adsorb the metal ions through ion-exchange mechanism.

2. Materials and methods

2.1. Preparation of radiotracer

The radiotracer of cerium used in this research was prepared by irradiating a known amount of Specpure $CeCl_3.6H_2O$ from Johnson & Matthey (UK), in a 10 MW swimming pool type reactor (PARR-1) at PINSTECH, Islamabad, for a specific duration at a neutron flux of 4.5×10^{13} cm^{-2} s^{-1}. After a suitable cooling time, the sample was dissolved in minimum amount of nitric acid and diluted to the desired volume with water.

2.2. Reagents

Low-rank Pakistani coal was collected from mines in the province of Punjab (Khushab, Makerwal). The sample was ground and sieved to a particle size of about 500 μm. The coal powder was activated at 300°C in a muffle furnace for 4 h to enhance the basicity of adsorbent. The activated sample was further treated with 2 M H_2SO_4 at room temperature for 2 h to oxidize the coal surface, increase the acidic character, remove the mineral components and improve the hydrophilicity of the surface. The acid treated coal was washed with water until the neutral pH of the filtrate. The washed coal sample was dried at 60°C till constant weight and stored in plastic container.

Buffer solutions of 1.0–12.0 pH, with an ionic strength of 0.1 M, were prepared by using appropriate volume of solutions of KCl and HCl (pH 1.0–3.0), CH_3COONa and CH_3COOH (pH 4.0–5.0), NH_4Cl and NH_4OH (pH 6.0–7.5), H_3BO_3, NaCl and NaOH (pH 8.0–10.0), and Na_2HPO_4 and NaOH (pH 11.0–12.0). All the reagents used were of analytical grade and were used as such. Distilled and deionized water was used in all experiments.

2.3. Adsorption measurements

A known amount of coal was taken in a 4 mL of standard acid solution or buffer solution of the required pH, along with a known aliquot of stock radiotracer solution in 16 mL culture tube with a screwed polyethylene cap. The contents were equilibrated on a mechanical shaker for 25 min and the supernatant solution was withdrawn. The radioactivities of the liquid phase were determined before and after the equilibration with a NaI well type scintillation counter (Canberra Inc., USA) coupled with a counter scalar (Nuclear Chicago, USA). The percentage adsorption of cerium ions from the solution was calculated using the following expression (1):

$$\%\ \text{age adsorption} = \frac{A_i - A_f}{A_i} \times 100 \quad (1)$$

where A_i is the initial radioactivity of cerium ions in the solution and A_f is the radioactivity of cerium ions in solution after equilibrium.

All the experiments were conducted at 298 ± 1 K and the reported values are the average of at least two independent measurements with an average relative standard deviation of ±3.5% unless otherwise specified.

3. Results and discussion

3.1. Characterization of adsorbent

The surface area of low-rank Pakistani coal sample was measured according to Brunauer–Emmett–Teller (BET) method by nitrogen adsorption at 77 K using Quanta chrome S1 BET surface area analyzer. Before nitrogen adsorption the sample was degased for 2 h at final pressure of 133.32×10^{-4} Pa. The bulk density, percentage porosity, pH and pH_{zpc} of the adsorbent were determined by using the reported methods [29,30] and the results are summarized in Table 1.

Table 1
Characteristics of low-rank Pakistani coal

Description of parameter	Value
Particle size	500 μm
Bulk density	2.0 g mL^{-1}
BET surface area	4.8 m^2 g^{-1}
Total pore volume	4.8×10^{-3} cc g^{-1}
Average pore diameter	4.0 nm
Porosity	53%
Organic content	81.61%
Ash content	18.39%
pH	5.10
pH_{zpc}	3.1

3.1.1. FTIR studies

The chemical modification of coal and cerium loaded coal was followed using Fourier transform infrared spectroscopy (FTIR). The FTIR spectra of low-rank coal, activated coal and cerium loaded activated coal are shown in Fig. 1. The absorption bands at 2,914, 1,736, 1,613, 1,439, 1,362, 1,211 and 1,027 cm^{-1} are attributed to the stretching of aliphatic C–H, carboxylic C=O, C=O, O–H bending of adsorbed H_2O, S=O stretching of sulfonic group, C–O and C–OH groups, respectively. Absorption bands at 430–470 and 516 cm^{-1} are due to mineral components. In case of activated coal the shifting of bands at 1,736, 1,362 and 1,211 cm^{-1} to 1,734, 1,365 and 1,217 cm^{-1} respectively, with enhanced intensity could be explained on the basis of increased number of carboxylic acid groups as a result of oxidation and incorporation of sulfate group on the surface of the coal. Following the cerium ion adsorption the FTIR spectra of coal exhibited changes in the peak position and relative intensities. The peaks at 1,734, 1,365 and 1,217 cm^{-1} were shifted to 1,730, 1,370 and 1,211 cm^{-1}, respectively, with decreased intensity, which suggest the binding of cerium ions with carboxylic acid and sulfonic acid groups present on the surface of the activated Pakistani coal.

3.1.2. Scanning electron microscopic (SEM) analysis

The SEM micrographs of coal and cerium adsorbed coal were recorded and are shown in Fig. 2. In the SEM image before adsorption the bright surface shows the rough and porous nature of the adsorbent, which is responsible for higher adsorption capacity. The loaded SEM micrograph describing the surfaces of particles after adsorption, it is clearly seen that the caves, pores and surfaces of coal were covered by cerium and as a result the surface has become smooth. It is evident that upon adsorbing cerium, the coal structure has changed. Similarly, the determined composition of coal by energy dispersive X-ray spectrum revealed the presence of C, O, Si and S. The presence of cerium energy peaks at 0.8, 4.83, 5.3 and 5.7 keV (Fig. 3) confirms the adsorption of cerium ions on the surface of coal.

3.2. Influence of mineral acid concentration

The chemical contact of the sorbent surfaces results in certain variation in sorption characteristics. Therefore, the adsorption characteristics of cerium (3.568×10^{-5} mol L^{-1}) was investigated in mineral acid solutions (HNO_3, HCl, H_2SO_4 and $HClO_4$) of varying concentration in the range of

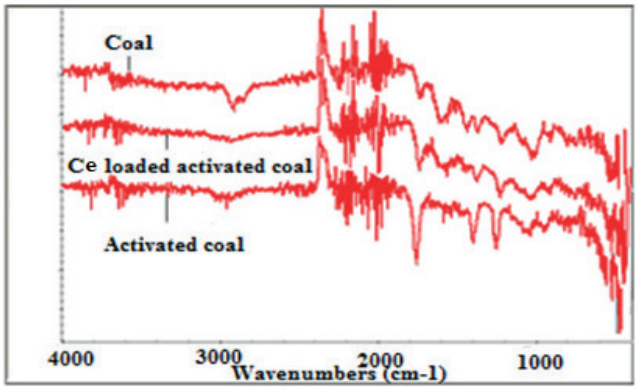

Fig. 1. FTIR spectrum of low-rank coal, activated coal and cerium loaded coal.

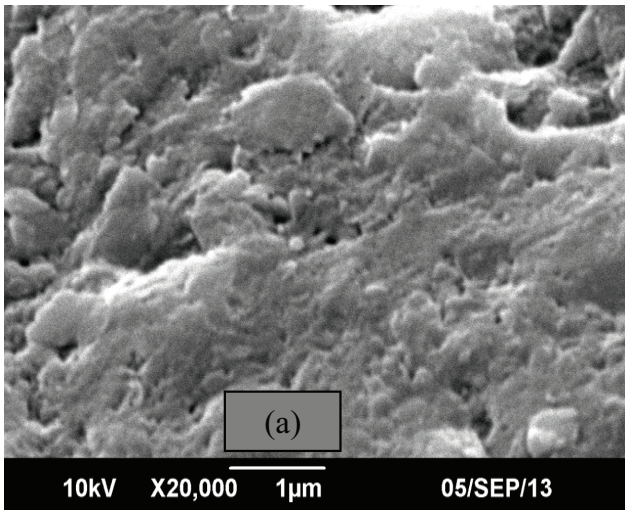

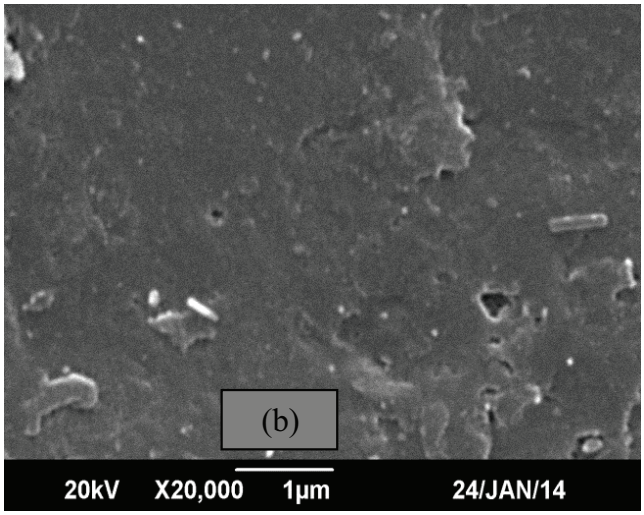

Fig. 2. SEM images of the low-rank coal before (a) and after (b) cerium adsorption.

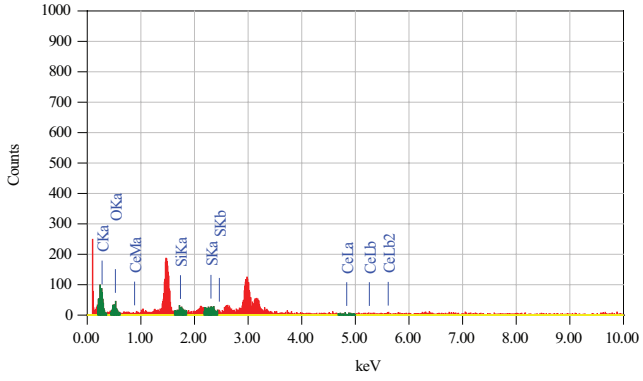

Fig. 3. Energy dispersive X-ray image of cerium loaded low-rank Pakistani coal.

0.0001–1.0 mol L^{-1} using optimized parameters. Fig. 4 shows that the adsorption of cerium ions decreases with an increase in acid concentration. This is due to the competition between the excess of H^+ ions in the medium and positively charged cerium ions. The same adsorption trend was observed for all the acids used in this study. Similar observations have also been reported for the adsorption of copper ions on low-rank Pakistani coal [31].

3.3. Influence of pH

The pH plays a significant role in the adsorption process by affecting the surface charge of the adsorbent, the extent of ionization and speciation of the adsorbate. Therefore, the effect of pH of the solutions on the adsorption efficiency of cerium ions was investigated at different pH ranging from 2.0 to 12.0, using 4 mL of 3.568×10^{-5} mol L^{-1} of cerium ion solution with 0.3 g of coal. The concentration of cerium ions and dose of 0.3 g of coal were selected arbitrarily and the results are presented in Fig. 5.

It was observed that there was a sharp increase in the adsorption of cerium ions from the initial pH values from 1 to 5, which gradually decreased with further increase in pH. At lower pH values, the surface of the adsorbent was highly associated with the hydrogen ions as compare with positively charged cerium ions. With the increase in the pH of the medium, the surface functional groups such as carboxyl, sulfonic are ionized and making the coal surface positively charged thus facilitating more adsorption of cerium ions on coal surface.

The adsorption of cerium ions on coal surface may be explained via cation exchange mechanism that can occur in the aqueous solution as follows:

$$m[\text{Coal–OH}] \rightleftharpoons m[\text{Coal–O}]^- + m\text{H}^+ \quad (2)$$

$$\text{M}^{n+} + m[\text{Coal–O}]^- \rightleftharpoons \text{M}[\text{Coal–}]_m^{(n-m)} \quad (3)$$

where [Coal–OH] is the activated coal surface; M^{n+} is the metal ions with n + charge and mH^+ is the number of protons released.

Since maximum adsorption of cerium ions occurred at pH 5, this optimum pH was selected for further experiments.

3.4. Effect of adsorbent dose

Effect of the weight of low-rank coal on the adsorption of Ce(III) ions was studied by varying the weight of coal from 0.1 to 0.5 g using 4 mL of 3.568×10^{-5} mol L^{-1} of cerium ion solution at 5.0 pH, with shaking time of 20 min and the results are shown in Fig. 6. It is clear from Fig. 6, that percentage adsorption was increased with an increase in the weight of coal and maximum adsorption was observed at 0.3 g of the adsorbent. With further increase in the weight of coal, there was no significant increase in adsorption. Therefore, 0.3 g of the coal was considered to be sufficient for the quantitative adsorption of cerium ion and was selected for further investigations.

3.5. Effect of shaking time

The effect of shaking time on removal of Ce(III) was studied by varying the time from 2 to 40 min using 4 mL of 7.136×10^{-5} mol L^{-1} of cerium ion solution at 5.0 pH with 0.3 g of coal and the results are shown in Fig. 7, which illustrates that the percentage adsorption of cerium ions was increased with the increase in shaking time. Maximum adsorption was observed at 25 min, after that no considerable increase was observed, therefore, this time was considered for further investigation.

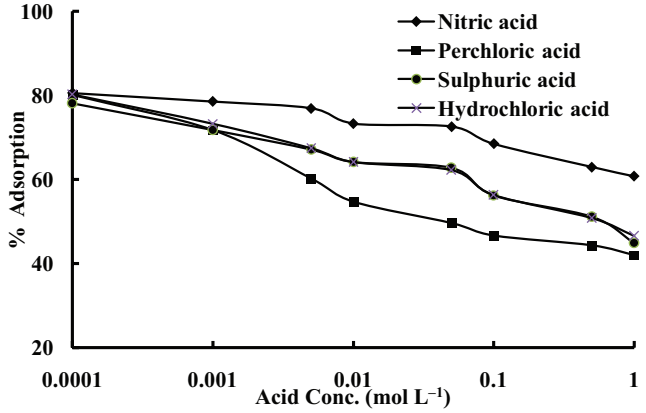

Fig. 4. Variation of adsorption of cerium ions on low-rank coal as a function of acid concentration.

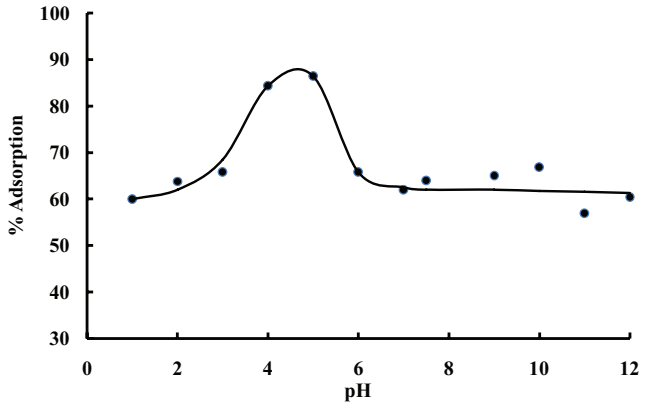

Fig. 5. Effect of pH on the adsorption of cerium ions on low-rank coal.

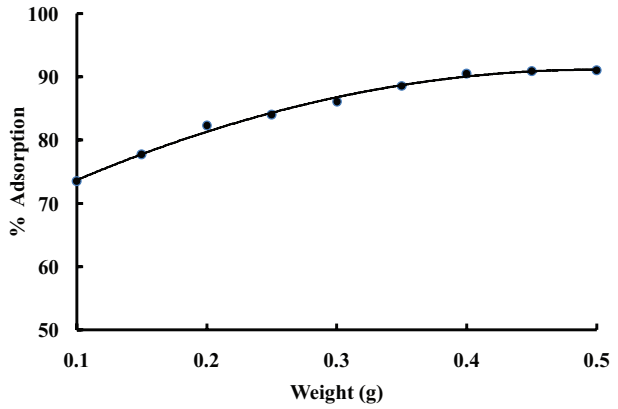

Fig. 6. Effect of coal dose on the adsorption of cerium ions.

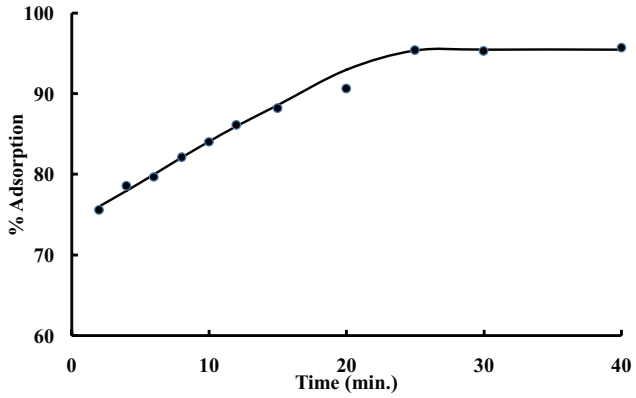

Fig. 7. Influence of equilibration time on the adsorption of cerium ions on low-rank Pakistani coal.

3.5.1. Kinetic studies

The adsorbates can move from the liquid medium to the surface binding sites of the adsorbent in different processes. Therefore, the time dependent adsorption data was subjected to the Morris–Weber expression [32]:

$$q_t = K_{\text{int}} t^{0.5} + C \tag{4}$$

where q_t is the concentration of cerium adsorbed at time t (mg g^{-1}); K_{int} is the intraparticle diffusion rate constant and C is the intercept.

The value of K_{int} was determined from the slope of the plot of q_t against $t^{0.5}$ (Fig. 8), which was found to be 2.0×10^{-3} mg g^{-1} min$^{-0.5}$, whereas the computed value of the intercept was 0.034.

To verify the adsorption process via either film diffusion or intraparticle diffusion mechanism the time dependent adsorption data was also subjected to the Reichenberg [33] Eq. (5):

$$X = \left(1 - \frac{6}{\pi^2}\right) e^{-B_t} \tag{5}$$

where

$$X = \frac{Q_t}{Q_e} = \frac{\text{Amount of metal adsorbed at time "}t\text{"}}{\text{Amount of metal adsorbed at equilibrium}}$$

The value of β_t is a mathematical function of X that can be calculated for each value of X by using Eq. (6):

$$\beta_t = -0.4977 \ln(1 - X) \tag{6}$$

The plot of β_t vs. time is a straight line (Fig. 9) with a correlation coefficient of 0.994 which indicates that the adsorption was controlled by film diffusion. It was also observed that the Reichenberg plot is not passing through origin indicating that the film diffusion is not the only mechanism involved during the adsorption of cerium ions on low-rank Pakistani coal.

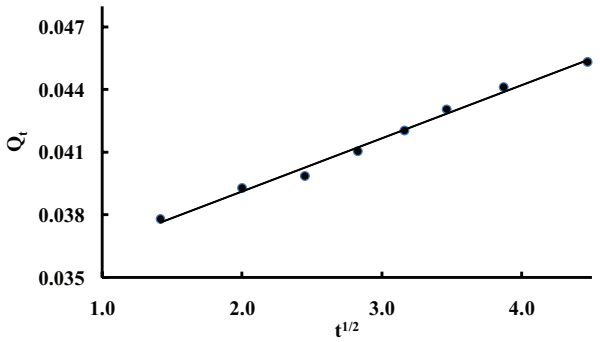

Fig. 8. Morris–Weber plot of cerium ions adsorption on low-rank Pakistani coal.

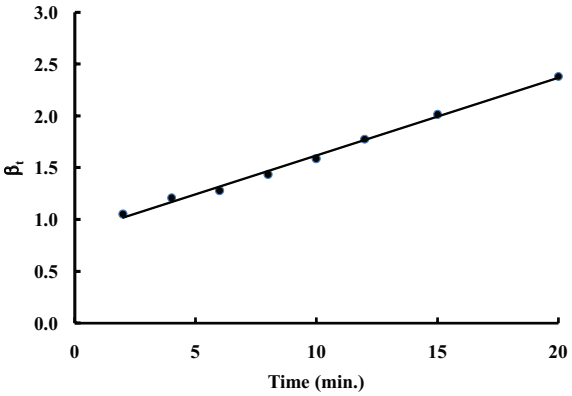

Fig. 9. Reichenberg plot of cerium ions adsorption on low-rank Pakistani coal.

In order to evaluate kinetic adsorption parameters the obtained kinetic adsorption data of cerium ions on coal was subjected to the first-order Lagergren (Eq. (7)) and pseudo-second-order (Eq. (8)) rate expressions using the linearized forms as:

$$\log\left(q_e - q_t\right) = \log q_e - \frac{K_1}{2.303} t \tag{7}$$

$$\frac{t}{q_t} = \frac{1}{K_2 q_e^2} + \frac{1}{q_e} t \tag{8}$$

where q_e is the amount of cerium adsorbed at equilibrium (mg g^{-1}), q_t is the amount of cerium adsorbed at any time t (mg g^{-1}), t is the time (min), K_1 is the rate constant of the first-order (min^{-1}) and K_2 is the rate constant of the pseudo-second-order (g mg^{-1} min^{-1}).

The straight lines were obtained by plotting $\log(q_e - q_t)$ against t and t/q_t vs. t, with correlation coefficients (R^2) of 0.995 and 0.999, respectively (Fig. 10). The determined kinetic parameters for the first-order and pseudo-second-order models are given in Table 2. The higher R^2 value and good correspondence between the determined (0.047 mg Ce g^{-1}) and the experimental (0.048 mg Ce g^{-1}) values of adsorption capacity confirm that the experimental kinetic data are in good agreement with the pseudo-second-order rate equation.

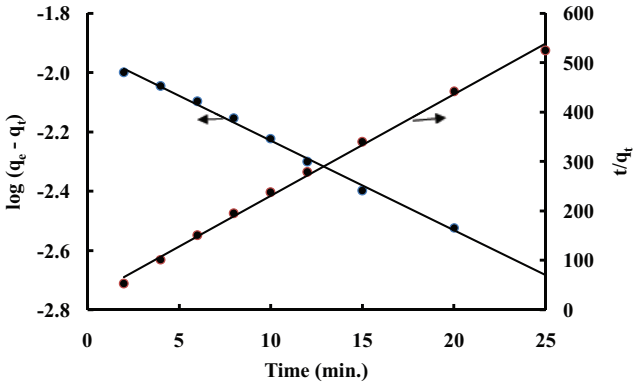

Fig. 10. Pseudo-first-order and pseudo-second-order plots for the adsorption of cerium ions on low-rank Pakistani coal.

Table 2
Kinetic data for the adsorption of cerium ions on low-rank Pakistani coal

Pseudo-first-order			Pseudo-second-order		
q_e (mg g^{-1})	K_1 (min^{-1})	R^2	q_e (mg g^{-1})	K_2 (g mg^{-1} min^{-1})	R^2
0.012	0.076	0.995	0.047 0.048[a]	25	0.998

[a]Experimentally calculated.

3.6. Effect of initial cerium ion concentration

The effect of cerium concentration on the adsorption efficiency was studied under the optimized conditions of contact time 25 min, adsorbent dose 0.3 g and the medium pH of 5.0. The initial concentration of cerium was varied from 3.568×10^{-5} to 6.423×10^{-4} mol L^{-1}. It was observed that the percentage adsorption was decreased with the increase in the concentration of cerium. This could probably be due to the availability of relatively lesser number of active sites in a fixed amount of coal at higher concentration of cerium.

3.6.1. Adsorption isotherms

The equilibrium adsorption isotherms describe the interactive behavior between an adsorbent and adsorbate, which is important to provide the basis for designing of an adsorption system. In the present work, the Freundlich, Langmuir and Dubinin–Radushkevich isotherm models were applied to the experimental data of cerium ion adsorption on low-rank Pakistani coal under the optimized parameters.

3.6.1.1. Freundlich isotherm The Freundlich relationship [34] was derived to interpret the multilayer adsorption of an adsorbate onto heterogeneous surface. Mathematically the Freundlich Eq. (9) is written as:

$$C_{\text{ad}} = KC_e^{\frac{1}{n}} \tag{9}$$

The logarithmic form of the above expression may be written as Eq. (10):

$$\log C_{\text{ad}} = \log K + \frac{1}{n}\log C_e \tag{10}$$

where C_{ad} is the amount of cerium sorbed (mol g^{-1}); C_e is the concentration of cerium in solution at equilibrium (mol L^{-1}); $1/n$ and K are Freundlich constants indicating the degree of heterogeneity or intensity of adsorption and adsorbent capacity, respectively. These constants were determined from the slope and intercept of the Freundlich isotherm (Fig. 11) and were found to be 0.381 and 5.152×10^{-2} m mol g^{-1}, respectively.

3.6.1.2. Langmuir isotherm The Langmuir adsorption isotherm model is commonly used to describe monolayer adsorption process onto a surface, where all sites have equal affinity for the metal ions. The linear form of Langmuir adsorption isotherm [35] may be expressed by the following Eq. (11):

$$\frac{C_e}{C_{\text{ad}}} = \frac{1}{Qb} + \frac{C_e}{Q} \tag{11}$$

where C_{ad} is the concentration of cerium sorbed at equilibrium (mol g^{-1}); C_e is the equilibrium concentration of cerium in solution (mol L^{-1}); Q and b are the Langmuir isotherm constants.

A plot of C_e/C_{ad} against C_e was a straight line (Fig. 12). This linear plot supports the validity of the Langmuir model in the present work. The values of Langmuir constants Q and b were calculated from the slope and intercept of the plot in Fig. 12 and were found to be 2.889×10^{-3} m mol g^{-1} and 14.072×10^3 dm^3 mol^{-1}, respectively.

The calculated adsorption capacity from Freundlich isotherm model (5.152×10^{-2} m mol g^{-1}) is higher as compared with the Langmuir isotherm model (2.889×10^{-3} m mol g^{-1}), which is in accordance with the assumptions of multilayer and monolayer adsorption, used during the derivation of these models, respectively.

3.6.1.3. Dubinin–Radushkevich isotherm In order to classify the physical or chemical adsorption, the adsorption data of cerium ions on low-rank Pakistani coal was subjected to the Dubinin–Radushkevich isotherm (D–R) model [36] by using the following expression (12):

$$C_{\text{ad}} = C_m \exp\left(-\beta \epsilon^2\right) \tag{12}$$

where C_{ad} is the amount of cerium sorbed on low-rank coal, C_m is the maximum amount of cerium that can be adsorbed on low-rank coal using the optimized experimental conditions, ε is Polanyi potential and β is a constant with a dimension of energy.

$$\varepsilon = RT\ln\left(1+\frac{1}{C_e}\right) \quad (13)$$

where R is the ideal gas constant; T is the absolute temperature; C_e is the equilibrium concentration of cerium in solution.

The linear form of D–R isotherm (Eq. (14)) can be written as:

$$\ln C_{ad} = \ln C_m - \beta\varepsilon^2 \quad (14)$$

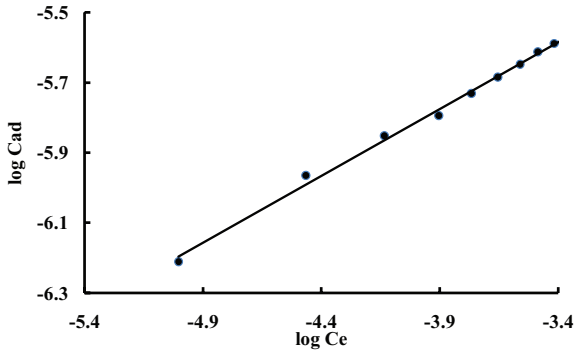

Fig. 11. Freundlich plot for the adsorption of cerium ions on low-rank Pakistani coal.

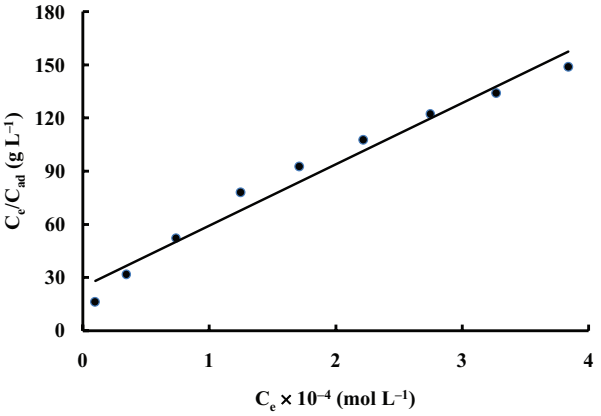

Fig. 12. Langmuir isotherm for the adsorption of cerium ions on low-rank Pakistani coal.

A straight line was obtained when $\ln C_{ad}$ was plotted against ε^2 (Fig. 13), indicating that cerium ions adsorption also obeys the D–R equation.

The value of slope (β) of the linear plot (Fig. 13) was found to be 3×10^{-3} K J^2 mol^{-2}. By substituting the value of β in Eq. (15) the mean adsorption energy (E_s) was determined as:

$$E_s = \frac{1}{(-2\beta)^{\frac{1}{2}}} \quad (15)$$

The values of E_s in the range of 1–8 and 8–14 kJ mol^{-1} are associated with physical and chemical adsorption, respectively [30,31]. The determined value of E_s for the present system was found to be 12.987 kJ mol^{-1}, indicating chemical adsorption of cerium ions on the surface of low-rank Pakistani coal. Similar observations have also been reported for the adsorption of copper ions on low-rank Pakistani coal [31].

3.7. Influence of temperature

The effect of temperature on the adsorption of 1.427×10^{-4} mol L^{-1} of cerium ions on coal was studied using the optimized parameters. The temperature was varied from 283 to 333 K and the results are shown in Table 3, which shows that the adsorption of cerium ions increases with the increase in temperature. van't Hoff plot, that is, $\ln K_c$ vs. $1/T$ (Fig. 14),

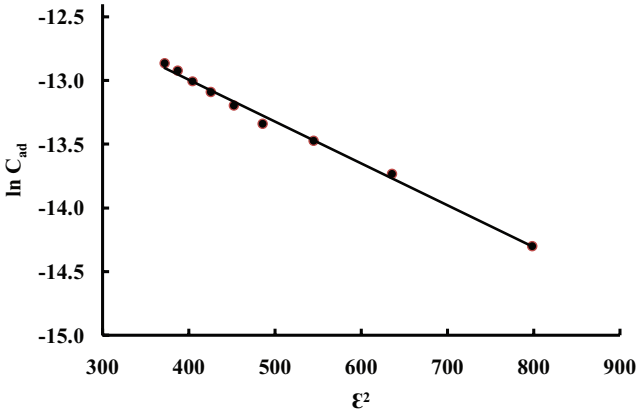

Fig. 13. Dubinin–Radushkevich isotherm plot for the adsorption of cerium ions on low-rank Pakistani coal.

Table 3
Adsorption behavior of cerium ions on low-rank Pakistani coal as a function of temperature

Temperature (K)	$1/T$ (K^{-1}) × 10^{-3}	Concentration adsorbed (mol L^{-1}) × 10^{-4}	Concentration in bulk (mol L^{-1}) × 10^{-5}	K_c	$\ln K_c$
283	3.534	1.007	4.197	2.400	0.875
293	3.413	1.082	3.454	3.131	1.141
303	3.300	1.144	2.834	4.035	1.395
313	3.195	1.219	2.078	5.869	1.770
323	3.096	1.285	1.424	9.018	2.199
333	3.003	1.324	1.029	12.866	2.555

Note: Weight of low-rank coal, 0.4 g; shaking time, 25 min; volume equilibrated, 4.0 cm^3; pH, 5; cerium ion concentration, 1.427×10^{-4} mol L^{-1}.

was used to find out ΔH and ΔS from its slope and intercept, respectively, by using the following expression (16):

$$\ln K_c = \frac{\Delta S}{R} - \frac{\Delta H}{RT} \tag{16}$$

where ΔH, ΔS, K_c, R and T are the change in enthalpy, change in entropy, equilibrium constant, gas constant and absolute temperature, respectively.

The equilibrium constant (K_c) was determined by using the relationship (17):

$$K_c = \frac{C_{eq.S}}{C_{eq.L}} \tag{17}$$

where $C_{eq.S}$ is the equilibrium concentration of cerium adsorbed on the coal (mg L^{-1}) and $C_{eq.L}$ is the equilibrium concentration of cerium in solution (mg L^{-1}).

ΔG and ΔS for the specific adsorption process have also been calculated using the expressions (18) and (19):

$$\Delta G = -RT \ln K_c \tag{18}$$

$$\Delta S = \frac{\Delta H - \Delta G}{T} \tag{19}$$

The determined values of ΔS, ΔG and ΔH have been summarized in Table 4. The negative values of ΔG represent that the adsorption of cerium on low-rank coal is a spontaneous process. The increase in the numerical value of $-\Delta G$ with the rise in temperature indicates that the adsorption process of cerium ions on coal is more favorable at higher temperatures. The positive values of enthalpy change (ΔH) represent the endothermic nature of the adsorption process. The positive value of entropy change (ΔS) reflects the increase in the randomness at solid–liquid interface during the adsorption of cerium ions on the coal surface.

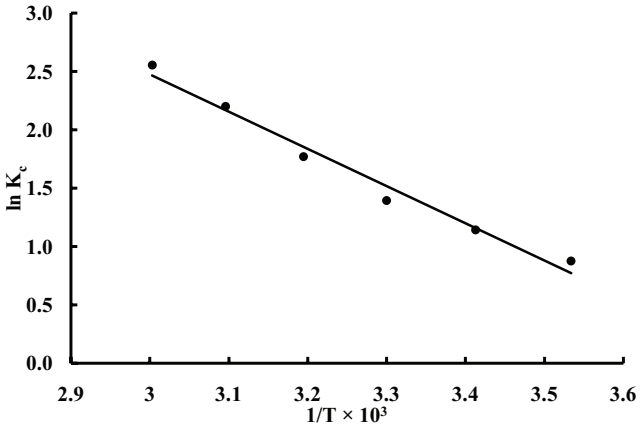

Fig. 14. van't Hoff plot for the adsorption of cerium ions on low-rank Pakistani coal.

3.8. Effect of coexistent ions

The presence of other cations and anions in the adsorptive phase may affect the environment and solution chemistry of the cerium ion, which influence the adsorption efficiency of low-rank coal. Therefore, using the optimized parameters the adsorption of 3.568×10^{-5} mol L^{-1} of cerium ions on coal was also studied in the presence of high concentrations of foreign ions. The anions were used as their sodium salts, while for cations the nitrate salts were used. The results are summarized in Table 5. The results show that adsorption efficiency of cerium on coal was decreased in the presence of K^+, Cr^{6+}, Al^{3+}, Fe^{3+}, Sb^{3+}, Co^{3+} and Ni^{2+} cations up to 6.3%, however, the adsorption of cerium was decreased due to the presence of F^-, SO_4^{2-}, S^{2-}, PO_4^{3-} and CN^- anions up to 32.94%. This decrease in the adsorption efficiency of cerium may be due to the competitor action of cations or the formation of stable complexes/compounds with anions for the active sites present on the surface of low-rank coal.

3.9. Application to the real system

In order to verify the applicability and efficiency of the optimized procedure on real samples, the removal of Ce^{3+} was checked from the ordinary tap water sample. Since no cerium was detected in the real tap water sample, therefore, 4.0 mL of sample was spiked with 3.568×10^{-5} mol L^{-1} of cerium ions. The pH of the medium was maintained by the addition of 1 mL of pH 5 buffer solution. The solution was equilibrated with 0.4 g of coal for 25 min. It was observed that 97% of the cerium was removed from the spiked tap water in a single step, indicating that low-ranked Pakistani coal has good potential to remove the cerium ions from such matrices.

3.10. Desorption studies

The desorption studies are important to evaluate the economic justification for regeneration and reuse of the adsorbent. Therefore, the desorption studies of adsorbed cerium ions on coal surface was also investigated. For this purpose 0.3 g of cerium loaded adsorbent was shaken with 1.0 mol L^{-1} of HNO_3 solution for 25 min, and the concentration of cerium ions in liquid phase was determined radiometrically. It was observed that 95% of the adsorbed cerium was transferred into acidic medium, indicating that the adsorbent can be reused after desorption of the adsorbed metal ions.

Table 4
Thermodynamic parameters for the adsorption of cerium ions on low-rank Pakistani coal

Temperature (K)	ΔG (kJ mol^{-1})	ΔH (kJ mol^{-1})	ΔS (kJ K^{-1} mol^{-1})
283	–2.060		0.101
293	–2.781		0.100
303	–3.514	26.596	0.099
313	–4.605		0.100
323	–5.906		0.101
333	–7.073		0.101

Table 5
Effect of cations and anions on the adsorption of 3.568×10^{-5} mol L^{-1} of cerium ions on low-rank Pakistani coal

Cations			Anions		
Ion	Concentration (mol L^{-1})	% Adsorption	Ion	Concentration (mol L^{-1})	% Adsorption
No ion	–	96.40	No ion	–	96.40
Na^{+}	1.088×10^{-3}	94.08	F^{-}	1.316×10^{-3}	78.88
K^{+}	6.410×10^{-4}	91.79	Cl^{-}	7.052×10^{-4}	92.00
Mg^{2+}	1.029×10^{-3}	93.46	Br^{-}	3.129×10^{-4}	93.99
Ca^{2+}	6.250×10^{-4}	96.09	SO_4^{2-}	2.604×10^{-4}	89.91
Al^{3+}	9.266×10^{-4}	92.63	S^{2-}	7.798×10^{-4}	87.85
B^{3+}	2.313×10^{-3}	95.42	NO_2^{-}	5.435×10^{-4}	91.85
Cr^{6+}	4.808×10^{-4}	90.10	PO_4^{3-}	2.632×10^{-4}	63.46
Fe^{3+}	4.477×10^{-4}	92.10	CN^{-}	9.615×10^{-4}	86.07
Sb^{3+}	2.053×10^{-4}	91.23	HCO_3^{-}	4.098×10^{-4}	91.72
Co^{2+}	4.242×10^{-4}	92.37	ClO_4^{-}	2.514×10^{-4}	90.22
Zn^{2+}	3.824×10^{-4}	93.56	NO_3^{-}	4.032×10^{-4}	95.24
Ni^{2+}	4.258×10^{-4}	91.18	$Citrate^{3-}$	2.514×10^{-4}	94.34
Mn^{2+}	4.551×10^{-4}	96.04	EDTA	6.721×10^{-5}	94.82

4. Conclusions

Coal has good potential for the adsorption of cerium from aqueous solutions. The adsorption of cerium on coal follows the pseudo-second-order rate expression. The cerium adsorption data followed the Langmuir, Freundlich and Dubinin–Radushkevich isotherms. The adsorption of cerium was increased with the increase in temperature. The thermodynamic parameters, that is, ΔG and ΔH represent spontaneity and endothermicity of cerium ion adsorption on coal. The adsorption of cerium from tap water sample indicates that the proposed method is efficient. On the basis of this study, it is concluded that the abundantly available, inexpensive coal may be used for the adsorption of cerium ions from aqueous media.

Acknowledgments

Tariq Javed would like to thank Higher Education Commission, Islamabad, Pakistan, for awarding an indigenous PhD scholarship and Pakistan Institute of Nuclear Science and Technology (PINSTECH), Islamabad, Pakistan, for providing necessary research facilities for the present studies.

References

[1] D. Humelnicu, G. Drochioiu, K. Popa, Bioaccumulation of thorium and uranyl ions on *Saccharomyces cerevisiae*, J. Radioanal. Nucl. Chem., 260 (2004) 291–293.
[2] K. Kondo, E. Kamio, Separation of rare earth metals with a polymeric microcapsule membrane, Desalination, 144 (2002) 249–254.
[3] T.P. Rao, V.M. Biju, Trace determination of lanthanides in metallurgical, environmental, and geological samples, Crit. Rev. Anal. Chem., 30 (2000) 179–220.
[4] M.A. Jakupec, P. Unfried, B.K. Keppler, Pharmacological properties of cerium compounds, Rev. Physiol. Biochem. Pharmacol., 153 (2005) 101–111.
[5] W.M. Higgins, A. Churilov, E. van Loef, J. Glodo, M. Squillante, K. Shah, Crystal growth of large diameter $LaBr_3$:Ce and $CeBr_3$, J. Cryst. Growth, 310 (2008) 2085–2089.
[6] H.K. Yoon, H.S. Moon, S.H. Park, J.S. Song, Y. Lim, N. Kohyama, Dendriform pulmonary ossification in patient with rare earth pneumoconiosis, Thorax, 60 (2005) 701–703.
[7] D. Schubert, R. Dargusch, J. Raitano, S.W. Chan, Cerium and yttrium oxide nanoparticles are neuroprotective, Biochem. Biophys. Res. Commun., 342 (2006) 86–91.
[8] A. Sharma, G. Talukder, Effects of metals on chromosomes of higher organisms, Environ. Mol. Mutagen., 9 (1987) 191–226.
[9] C.C. Kartha, J.T. Eapen, C. Kutty, V.R. Radhakumary, K. Ramani, A.V. Lal, Pattern of cardiac fibrosis in rabbits periodically fed a magnesium-restricted diet and administered rare earth chloride through drinking water, Biol. Trace Elem. Res., 63 (1998) 19–30.
[10] N. Um, T. Hirato, Precipitation of cerium sulfate converted from cerium oxide in sulfuric acid solutions and the conversion kinetics, Mater. Trans., 53 (2012) 1986–1991.
[11] B.N. Kokare, A.M. Mandhare, M.A. Anuse, Liquid–Liquid extraction of cerium(IV) from salicylate media using N-n-octylaniline in xylene as an extractant, J. Chil. Chem. Soc., 55 (2010) 431–435.
[12] S. Radhika, B. Kumar, N. Kantam, M. Lakshmi, R.B. Ramachandra, Solvent extraction and separation of rare earths from phosphoric acid solution with TOPS 99, Hydrometallurgy, 110 (2011) 50–55.
[13] D. Fontana, L. Pietrelli, Separation of middle rare earths by solvent extraction using 2-ethylhexylphosphonic acid mono-2-ethylhexyl ester as an extractant, J. Rare Earths, 27 (2009) 830–833.
[14] L. Jelinek, W. Yuezhou, M. Kumagai, Adsorption of Ce(IV) anionic nitrato complexes onto anion exchangers and its application for Ce(IV) separation from rare earths(III), J. Rare Earths, 24 (2006) 385–391.
[15] M.E. Mohammad, S. Muttucumaru, Review of pollutants removed by electrocoagulation and electrocoagulation/flotation processes, J. Environ. Manage., 90 (2009) 1663–1679.
[16] D.E. Chirkst, O.L. Lobacheva, I.V. Berlinskii, M.A. Sulimova, Recovery and separation of Ce^{3+} and Y^{3+} ions from aqueous solutions by ion flotation, Russ. J. Appl. Chem., 82 (2009) 1370–1374.
[17] O.L. Lobacheva, I.V. Berlinskii, O.V. Cheremisina, Solvent sublation and ion flotation in aqueous salt solutions containing Ce(III) and Y(III) in the presence of a surfactant, Russ. J. Appl. Chem., 87 (2014) 1863–1867.
[18] O.L. Lobacheva, N.V. Dzhevaga, D.E. Chirkst, Solvent sublation of cerium ions from dilute aqueous solutions, Russ. Chem. Bull., 61 (2012) 962–965.

[19] G.K. Tahyali, S. Sert, B. Etinkaya, S. Inan, M. Eral, Factors affecting lanthanum and cerium biosorption on *Pinus brutia* leaf powder, Sep. Sci. Technol., 45 (2010) 1456–1462.
[20] S. Sert, C. Kutahyali, S. Inan, Z. Talip, B. Cetinkaya, M. Eral, Biosorption of lanthanum and cerium from aqueous solutions by *Platanus orientalis* leaf powder, Hydrometallurgy, 90 (2008) 13–18.
[21] R. Rusnadi, B. Buchari, M.B. Amran, D. Wahyuningrum, Cerium adsorption using 1-phenyl-3-methyl-4-benzoyl-5-pyrazolone (HPMBP) loaded calcium alginate beads, Int. J. Eng. Res. Appl., 2 (2012) 496–499.
[22] M.A. Gelee, H. Kamal, Adsorption of Ce(III) from aqueous solution using acrylic acid grafted low density polyethylene films, N. Y. Sci. J., 4 (2011) 28–34.
[23] M. Torab-Mostaedi, Biosorption of lanthanum and cerium from aqueous solutions using tangerine (*Citrus reticulata*) peel: equilibrium, kinetic, and thermodynamic studies, Chem. Ind. Chem. Eng., 19 (2013) 79–88.
[24] M.S. Sayed, A.S. Abdel-Razek, T.M. El-Morsy, M.A. El-Nawawy, R.M. Abd-Allah, Adsorption studies on the uptake of Ce(III) from liquid wastes using kaolin clay, J. Radiat. Res. Appl. Sci., 4 (2011) 807–826.
[25] C.H. Ooi, A. Ito, T. Otake, F.Y. Yeoh, Cerium removal by activated carbon derived from palm kernel shell, Adv. Mater. Lett., 8 (2017) 145–149.
[26] S.S. Dubey, B.S. Rao, Removal of cerium ions from aqueous solution by hydrous ferric oxide – a radiotracer study, J. Hazard. Mater., 186 (2011) 1028–1032.
[27] S.S. Dubey, B.S. Rao, Removal of cesium and cerium ions from aqueous solution by hydrous manganese oxide – a radiotracer study, J. Pharm. Res., 5 (2012) 4774–4779.
[28] F. Huanga, F. Yia, Z. Wang, H. Li, Sorptive removal of Ce(IV) from aqueous solution by bentonite, Procedia Environ. Sci., 31 (2016) 408–417.
[29] G. Vijayakumar, R. Tamilarasan, M. Dharmendirakumar, Adsorption, kinetic, equilibrium and thermodynamic studies on the removal of basic dye rhodamine-B from aqueous solution by the use of natural adsorbent perlite, J. Mater. Environ. Sci., 3 (2012) 157–170.
[30] Y. Zhang, A.E. Ghaly, B. Li, Physical properties of rice residues as affected by variety and climatic and cultivation conditions in three continents, Am. J. Appl. Sci., 9 (2012) 1757–1768.
[31] T. Javed, N. Khalid, M.L. Mirza, Adsorption characteristics of copper ions on low-rank Pakistani coal, Desal. Wat. Treat., 59 (2017) 181–190.
[32] W.J. Weber, J.C. Morris, Kinetics of adsorption on carbon from solution, J. Sanit. Eng. Div. Am. Soc. Civ. Eng., 89 (1963) 31–63.
[33] D. Reichenberg, Properties of ion-exchange resins in relation to their structure. III. Kinetics of exchange, J. Am. Chem. Soc., 75 (1953) 589–597.
[34] U. Freundlich, Die adsorption in lusungen, J. Phys. Chem., 57 (1906) 385–470.
[35] I. Langmuir, The adsorption of gases on plane surfaces of glass, mica and platinum, J. Am. Chem. Soc., 40 (1918) 1361–1403.
[36] M.M. Dubinin, E.D. Zaverina, L.V. Radushkevich, Sorption and structure of active carbons. I. Adsorption of organic vapours, Zh. Fiz. Khim., 21 (1947) 1351–1362.